A new joint application of non-invasive remote sensing techniques for structural health monitoring



2012 J. Geophys. Eng. 9 S53

(http://iopscience.iop.org/1742-2140/9/4/S53)

IOP Publishing Journal of Geophysics and Engineering
J. Geophys. Eng. **9** (2012) S53–S63 doi:10.1088/1742-2132/9/4/S53

# A new joint application of non-invasive remote sensing techniques for structural health monitoring

**T A Stabile, A Giocoli, A Perrone, A Palombo, S Pascucci and S Pignatti**

Consiglio Nazionale delle Ricerche, Istituto di Metodologie per l'Analisi Ambientale (CNR-IMAA), Tito, PZ, Italy

E-mail: tony.stabile@imaa.cnr.it

Received 24 February 2012
Accepted for publication 11 June 2012
Published 9 August 2012
Online at stacks.iop.org/JGE/9/S53

**Abstract**
This paper aims at analysing the potentialities of a new technological approach for the dynamic monitoring of civil infrastructures. The proposed approach is based on the joint use of a high-frequency thermal camera and a microwave radar interferometer to measure the oscillations due to traffic excitations of the Sihlhochstrasse Bridge, Switzerland, which was selected as test bed site in the ISTIMES project (EU—Seventh Framework Programme). The good quality of the results encourages the use of the proposed approach for the static and dynamic investigation of structures and infrastructures. Moreover, the remote sensing character of the two applied techniques makes them particularly suitable to study structures located in areas affected by natural hazard phenomena, and also to monitor cultural heritage buildings for which some conventional techniques are considered invasive. Obviously, their reliability needs further experiments and comparisons with standard contact sensors.

**Keywords:** remote sensing, radar interferometry, high-frequency thermography, thermal imaging, structure displacement analysis, structural health monitoring

(Some figures may appear in colour only in the online journal)

## 1. Introduction

Great attention has been paid in the last decades to the economic and social effects of ageing, worsening and extreme events on civil infrastructures (Chang *et al* 2003). As changes to the material and/or geometric properties of a structure can severely affect its performance, early warnings on damage or deterioration prior to costly repair or even catastrophic collapse (Mucciarelli *et al* 2011) have been recognized by administrative authorities. The study of the behaviour of real or designed civil infrastructures during strong seismic excitations (e.g. Martire *et al* 2010, 2012, Picozzi *et al* 2010) or simply during their entire life (e.g. Pines and Aktan 2002) has become an important issue because it implies significant life safety and economic benefits.

In recent years, most research efforts have gone into the development of methods (Farrar and Worden 2007 and references therein) and techniques (Ko and Ni 2005 and references therein) for structural health monitoring (SHM) of civil infrastructures in order to retrieve a valid substitute for more traditional methods such as visual inspection or the tap test. In this sense, a number of new research projects has been funded to improve the damage detection methods including the use of innovative signal processing, new sensors and control theory (Li *et al* 2004, Ali *et al* 2012). In these projects, great attention is paid to the application of ground-based remote sensing electromagnetic sensors that can provide information on the dynamic characteristics of infrastructures without the need to install sensors directly on the structure surface (Proto *et al* 2010). These sensors can be divided into optical systems, such as the global positioning system (Nickitopoulou *et al* 2006), laser-based systems (Cunha and Caetano 1999), vision-based systems (Lee and Shinozuka 2006), thermal systems, such as the infrared thermal camera (Brown and Hamilton

  

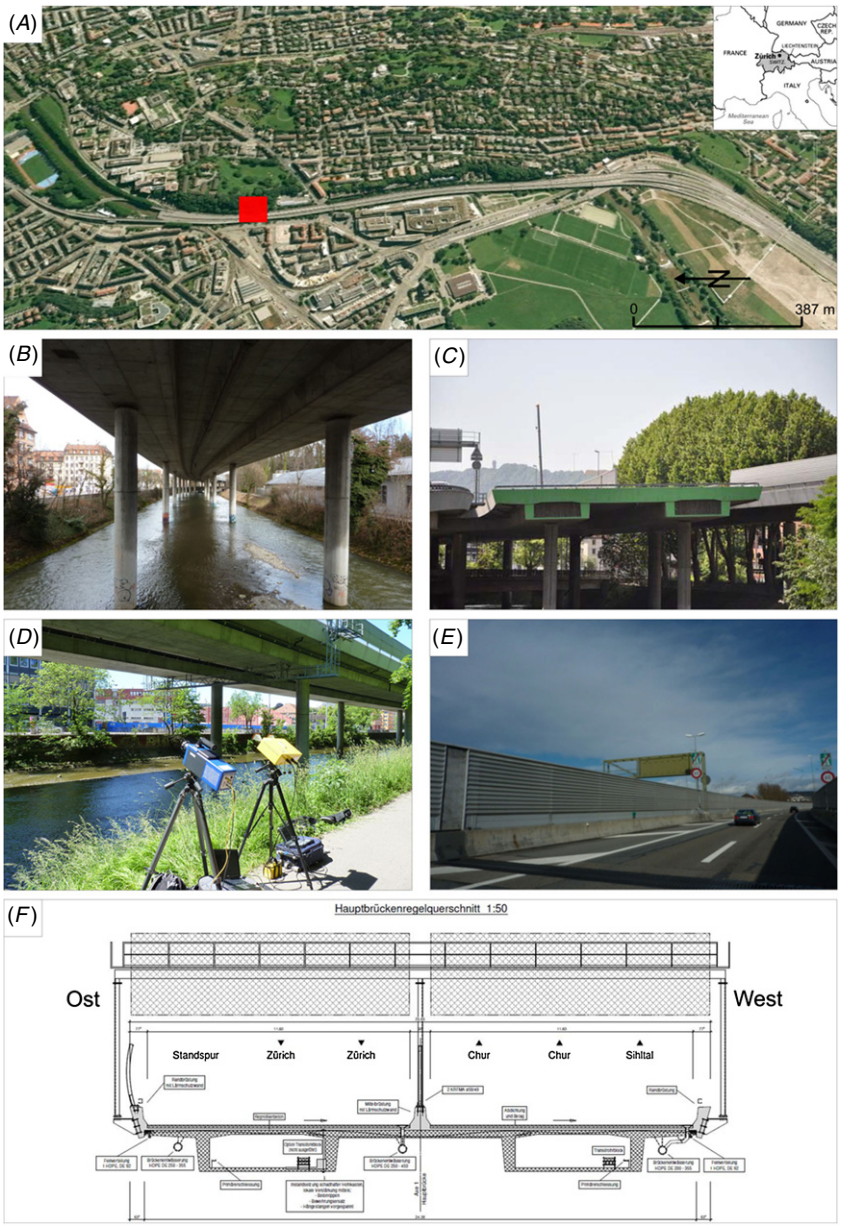


**Figure 1.** (*A*) Sihlhochstrasse Bridge test site: the box highlights the location of measurements; (*B*) piles in river Sihl; (*C*) northern end of main bridge; (*D*) FLIR camera (on the left) and IBIS-S (on the right) sensors at work; (*E*) sound insulating walls; (*F*) main cross section.

2010, Palombo *et al* 2011) and microwave systems, such as the microwave radar interferometer (Farrar *et al* 1999) recently developed into the image by interferometric survey of structures (IBIS-S) system (Pieraccini *et al* 2004, Gentile and Bernardini 2009).

Some of these sensors have been jointly applied in the framework of the 'integrated system for transport infrastructures surveillance and monitoring by electromagnetic sensing' (ISTIMES) project with the aim to test their ability to detect changes in a structure's behaviour (e.g., Minardo *et al* 2012). In particular, in this paper the main advantages and drawbacks related to the application of high-frequency thermal camera (FLIR SC7900-VL) and microwave radar interferometer (IBIS-S) systems to investigate Sihlhochstrasse Bridge (Zurich, Switzerland) are discussed. Both instrument datasets were recorded at the same time and at the same position in front of the target of interest (figure 1) in order to perform a direct comparison to each other.

IBIS-S sensor has been already successfully applied for the monitoring of a wide variety of structures, such as tracking the vibration of bridges excited by vehicular traffic (Pieraccini *et al* 2007, Gentile and Bernardini 2008), the monitoring of the displacements of heritage architectural structures (Atzeni *et al* 2010), for deflection measurements on vibrating stay cables (Gentile 2010) and for in-field dynamic monitoring of engineering structures (Pieraccini *et al* 2008, Rödelsperger *et al* 2010). This sensor can measure the displacement of different points of target placed along the line of sight (LOS) with a sensitivity of 0.01–0.02 mm comparable to commercial accelerometers. IBIS-S can work day and night in all weather

conditions and can be positioned up to a distance of 1 km from the target to be investigated, reducing hazards for operators.

The thermal infrared (TIR) camera represents a flexible and rapid tool to be used both for low-frequency long time series acquisitions, allowing analysis of structure homogeneity and the cohesion of the surface structure layer with the subsurface ones, and for high-frequency acquisitions for a fast diagnostics at different spatial resolutions, as it can be easily mounted on a plane and acquire a huge number of data. Therefore, the infrared technology (IRT) can acquire high-frequency long time series day and night with a high sensitivity for recording the vibrations (Palombo *et al* 2011) and, at the same time, it allows us to obtain low-frequency images to be used for a real time in-depth inspection of the areas of a structure more interested by superficial discontinuities and sub-surface defects (Maierhofer *et al* 2006) in the structure such as initial detachments and water infiltration and the inner structure itself. The expected limits for the application of the thermal camera are mostly related to the weather conditions, in particular the wind that forces different configurations of the measuring platform, i.e. the equipment must be better fixed to the ground in order to isolate the sensors from the source of disturbance.

The joint application of the non-invasive remote sensing FLIR thermal camera and IBIS-S sensor introduces a totally new methodology for the static and dynamic monitoring of structures with many advantages over traditional techniques such as those based on accelerometers, including (a) completely non-invasive monitoring, with no need to close the structure or to have access to it; (b) day-and-night workability; (c) easy and fast installation and operation; (d) two-dimensional simultaneous mapping of all displacements detected on the structure. The dynamic displacement data collected by the use of the FLIR thermal camera and the IBIS-S sensor were used to also provide resonant frequencies of the Sihlhochstrasse Bridge, which are very important for the SHM since their changes over time represent indicators for potential structural degradation.

## 2. The Sihlhochstrasse Bridge test bed

The Sihlhochstrasse Bridge located in Zurich is one of the largest bridges in Switzerland with a length of 1.5 km and it was selected as a test bed site in the ISTIMES project (funded by the European Commission in the frame of a joint Call 'ICT and Security' of the Seventh Framework Programme) for its size and its structural complexity and because EMPA (Swiss Federal Laboratories for Materials Science and Technology) has carried out several bridge-related research projects in cooperation with the FEDRO (Swiss Federal Roads Authority). The collaboration with EMPA and FEDRO allowed us to use the Sihlhochstrasse Bridge for testing and demonstration purposes within the framework of the ISTIMES project.

In particular, Sihlhochstrasse is a bridge with a length of about 1.5 km (without ramps) situated in Zurich on the motorway A3 (figure 1(*A*)). It was completed in 1973 and major rehabilitation was carried out between 2000 and 2001. The Sihlhochstrasse Bridge is a reinforced concrete bridge equipped with girder boxes. The main cross section is presented in figure 1(*F*). The bridge deck has a width of 24.38 m and is covered with asphalt pavement and a sealing between asphalt and concrete. In addition to the tendons in the girder boxes, there are also tendons orthogonal to the bridge axis in the bridge deck itself. There are concrete parapets on both sides and in the centre of the bridge deck. The bridge is equipped with metal sound insulating walls (figure 1(*E*)). The main bridge is carried by pairs of concrete piles with oval cross section that are standing in the river Sihl (figure 1(*B*)). A special feature of the Sihlhochstrasse Bridge is its northern end (figure 1(*C*)) where the originally planned continuation of the structure was abandoned due to a change in public opinion.

For a direct comparison of the two methods, a synchronized application (i.e. at the same time, position and distance of 15 m) has been done for the Sihlhochstrasse Bridge test bed. An example of the instrumentation configuration at work at the bridge test bed is reported in figure 1(*D*).

## 3. Basic concepts and methods

The IBIS-S sensor can provide the displacement information of the monitored structure along the radar's LOS; hence, it is possible to compute resonant frequencies related to both vertical and horizontal oscillations if measurements are carried out with a tilted LOS. Anyway, sometimes this could be considered also a limitation if we want to separate the contributions from different directions. In this case, two such systems orthogonal to each other must be simultaneously used, or the same instrument must be placed in different positions with the loss of synchronization.

A promising alternative solution to this problem comes from an experiment carried out in October 2010 at Montagnole (French Alps), in the framework of the ISTIMES project, where the progressive damage in different stages of a concrete beam was tested by means of falling blocks (Palombo *et al* 2011). In that work, the resonant frequencies obtained from the vertical oscillations of the concrete beam after each impact were measured independently by the IBIS-S instrument and the high-frequency imagery (HFI) FLIR thermal camera, which provided comparable results.

Indeed, even if the thermal camera is primarily suited for the detection and characterization of alterations and defects in the near surface of structures (Maierhofer *et al* 2006), its use as a HFI camera gives the opportunity of measuring vibrations of the structure in the plane orthogonal to the LOS of the camera.

The method proposed in this work considers the joint application of the FLIR camera and the IBIS-S sensor to the measurement of the displacement and resonant frequencies of the bridge along orthogonal directions.

In the following, a description of the sensor characteristics and of the techniques used by the sensors to give the measurement of the displacement of structures is introduced.

### *3.1. The microwave radar interferometer (IBIS-S sensor)*

The IBIS-S microwave radar consists of a sensor module installed on a tripod with a 3D rotating head. The two horn

antennas of the sensor module transmit the electromagnetic signals in the Ku frequency band of 16.75 ± 0.30 GHz, and receive the echoes from the targets to be processed in order to compute the displacement time histories of different points of the investigated structure with a sensitivity of 0.01–0.02 mm. A maximum sampling frequency of 200 Hz of the displacement can be reached with the IBIS-S instrument.

This innovative radar system, widely described in previous works (e.g. Gentile 2010 and references therein), is based on the stepped-frequency continuous wave (SF-CW) technique (Taylor 2001) and on the differential interferometric technique (Henderson and Lewis 1998); the former provides the system with a range resolution capability and the latter allows the system to evaluate the displacement response of each target detected in the illuminated scenario.

The range resolution $\Delta r$ is a measure of the minimum distance between two targets at which they can still be detected individually in distance along the radar's LOS. It is related to the pulse duration $\tau$ by the following relation (Taylor 2001):

$$\Delta r = \frac{c\tau}{2} = \frac{c}{2B}, \tag{1}$$

where $B = 1/\tau$ is the frequency bandwidth of the transmitted electromagnetic wave, and $c$ is the speed of light. The SF-CW technique consists in the synthesis and transmission of a burst of $N$ monochromatic tones equally and incrementally spaced in frequency (with a fixed frequency step of $\Delta f$) leading to a work bandwidth $B$:

$$B = (N-1)\Delta f. \tag{2}$$

The $N$ monochromatic tones sample the scenario in the frequency domain similarly to a short pulse with a large bandwidth $B$. Then, by considering equation (1), it is possible to have a bandwidth $B$ large enough to obtain the desired range resolution, which is 0.5 m for the IBIS-S system. This means that the sensor can distinguish two different targets if their relative distance is greater than 0.5 m.

From echoes coming from different range bins (i.e. different range resolution areas), it is possible to process phase information at regular time intervals to find any radial displacement $d_p$ (i.e. the displacement along the LOS) occurring between one emission and the next for the entire measurement period. This processing can be done by using the differential interferometric technique (Henderson and Lewis 1998, Gentile and Bernardini 2008) as follows:

$$d_p \propto \frac{\lambda}{4\pi}\Delta\phi, \tag{3}$$

where $\Delta\phi$ is the phase shift between one emission and the next and $\lambda$ (1.79 ± 0.03 cm) is the wavelength of the electromagnetic signal. The measured radial displacement time history $d_p(t)$ is related to the vertical $V(t)$ and horizontal $H(t)$ displacements of the target by the following relation:

$$d_p(t) = V(t)\sin(\theta) + H(t)\cos(\theta), \tag{4}$$

with $\theta$ being the LOS angle computed counterclockwise from the horizontal axis (see figure 2). If one of the two quantities on the right-hand side of equation (4) is negligible with respect to the other or is known, the other quantity can be obtained from the radial displacement $d_p(t)$ by a simple geometric projection.

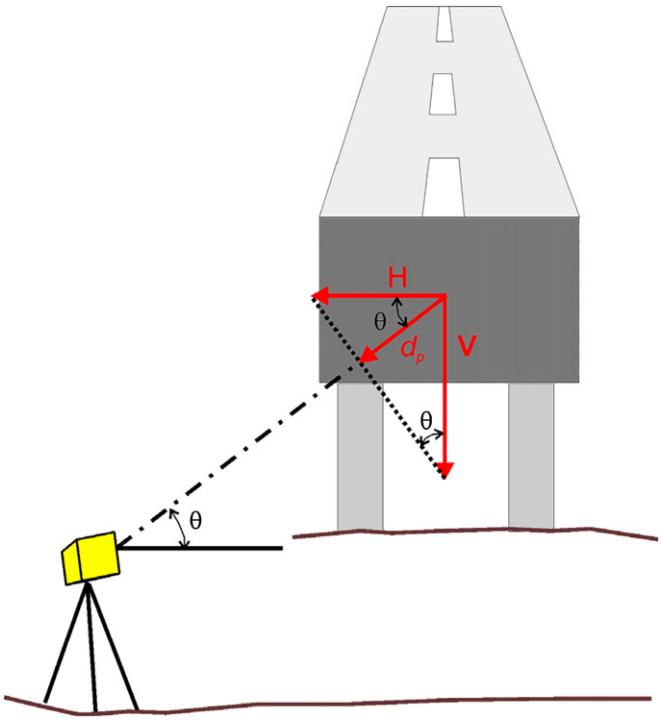


**Figure 2.** Pictorial figure describing the operating principle of the ground-based radar interferometer (IBIS-S) according to equation (4).

### *3.2. The HFI thermal camera (FLIR camera)*

The thermal camera technology is a non-destructive diagnostic technique commonly used in different applications (Malone *et al* 2005, Pascucci *et al* 2008, Ha *et al* 2012) mainly applied for the detection and characterization of defects in the structures' subsurface (Maierhofer *et al* 2006) and for the displacement monitoring and verification of the structural integrity of buildings and structures (Proto *et al* 2010). This type of analysis combined with other techniques is also used for the structural status monitoring and the application of vibration-based damage detection techniques (Doebling *et al* 1996). For this study high-frequency LWIR (7.7–11.5 $\mu$m) imagery acquisitions (Palombo *et al* 2011) were used for retrieving vibrations for the Sihlhochstrasse Bridge.

Concerning the high sensitivity TIR instrumentation, we used for this study a FLIR SC7900-VL thermal camera (LWIR; 7.7–11.5 $\mu$m). The FLIR camera has an integration range from 10 $\mu$s to 10 ms, which incorporates a high quantic efficiency MCT focal plane array thus ensuring a very high radiometric resolution with a noise equivalent temperature difference (NEDT) < 25 mK. The frame rates are up to 600 frames per second (FPS) in a sub-windowing mode. Due to the high sensitivity characteristics of the applied FLIR camera, it is possible to obtain excellent thermal images with low crosstalk between adjacent pixels; therefore, we do not consider in this study the influence of the crosstalk of neighbouring pixels that typically affects optical/electrical sensors (Rehm *et al* 2005).

For the experiment conducted in this study, the minimum requirements for an IR camera system to perform the proposed investigations are a frame rate of up to 50 Hz, whereas

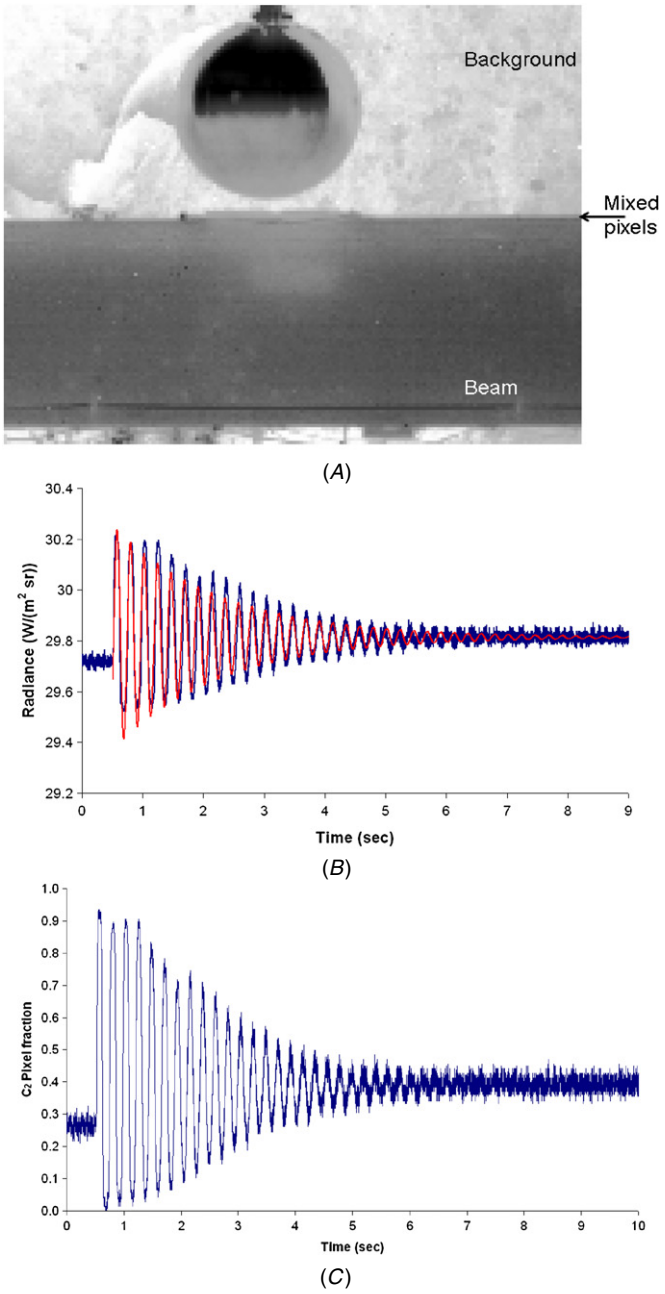


**Figure 3.** (*A*) Example of a frame acquired by FLIR camera. The image frame depicts the heavy load of the controlled Montagnole experiment just before the impact on the concrete beam. The black arrow indicates the mixed pixels (i.e. background and beam) used for calculating the oscillation frequency after the impact. (*B*) Example of a graph showing the radiance oscillations acquired by the FLIR camera on Montagnole. The graph shows the under-dumping decay attained for the radiance of the *i-pixel* occupied by the beam (the superimposed line depicts the theoretical dumper oscillator). (*C*) the $C_2$ pixel fraction value calculated for the Montagnole experiment.

regarding the minimum NEDT, it is scene dependent thus not quantifiable *a priori*.

These requirements have been also chosen considering the results attained for a controlled experiment performed in Montagnole (figure 3) within the ISTIMES project, in which the drops of a heavy iron ball on a cement beam were used as mechanical solicitation to measure the dynamic response of the beam (Palombo *et al* 2011). For the Montagnole case study, we used a simple model by considering the behaviour of the beam as that of a damped harmonic oscillator where the equation describing the oscillation is

$$z(t) = A_0\, \mathrm{e}^{-\varsigma\omega_0 t}\, \sin(\sqrt{1} - \varsigma\omega_0 t + \varphi), \tag{5}$$

where $A_0$ is the amplitude and $\varphi$ is the phase that dictates the initial conditions, $w_0$ is the undamped angular frequency of the oscillator and $z$ is the damping ratio that is given, respectively, by

$$\begin{aligned} \omega_0 &= \sqrt{\tfrac{k}{m}} \\ \varsigma &= \tfrac{c}{2m\omega_0}, \end{aligned} \tag{6}$$

where $k$ is the elastic constant, $m$ is the mass and $c$ is the viscous damping coefficient.

The value of $\zeta$ determines the behaviour of the system; in fact, the damped harmonic oscillator can be (a) for $\zeta > 1$, the system is represented by exponential decays; (b) for $\zeta = 1$, the system returns to equilibrium as quickly as possible without oscillating; (c) for $\zeta < 1$, the system is represented by an underdamped harmonic oscillator (figure 3(*B*)).

The thermal imagery acquisitions were used to calculate the oscillation frequency of the monitored structure as derived from the difference between the structure temperature and the background temperature. The oscillation retrieval technique is based on the presence of pixels composed of both the monitored structure and the background, i.e. mixed pixels, further labelled as *i-pixel* (figures 3(*A*) and 4(*B*)). The pixel used for the oscillation measurement was selected on the basis of its composition, i.e. a pixel composed of ∼50% of background and 50% of target.

As the assumption of this study is a linear relationship between the signals coming from (*i*) the background, (*ii*) target and (*iii*) mixed pixels, we used the radiance values instead of the temperatures as this can ensure the linearity behaviour. The method is based on the presence of mixed pixels composed of both the beam and the background as shown in figure 3(*A*), labelled as *i-pixel*. The *i-pixel* radiance measured by the FLIR camera depends on both the time-varying radiance relative to the structure and the background. In this case, the time was not considered as the equations are referred to a single frame each time thus considering as implied the time dependence. The following equations were used to describe the pixel radiance oscillation:

$$c_1 L_b + c_2 L_n = L_{\mathrm{mix}} \tag{7}$$

$$c_1 + c_2 = 1, \tag{8}$$

where $c_1$ and $L_b$ are the fraction of the *i-pixel* of the background and its radiance, respectively; $c_2$ (figure 3(*C*)) and $L_n$ are the fraction of the *i-pixel* of the structure and its radiance, respectively. $L_{\mathrm{mix}}$ is the radiance measured by the camera for the *i-pixel*. Equation (7) represents the linear mixing of the radiances of the monitored structure and the background, while equation (8) is the constraint used for the total pixel fraction.

Such a technique allows measuring the dynamic displacement of the structure by using the variation in time of the mixed pixel radiance in the investigated

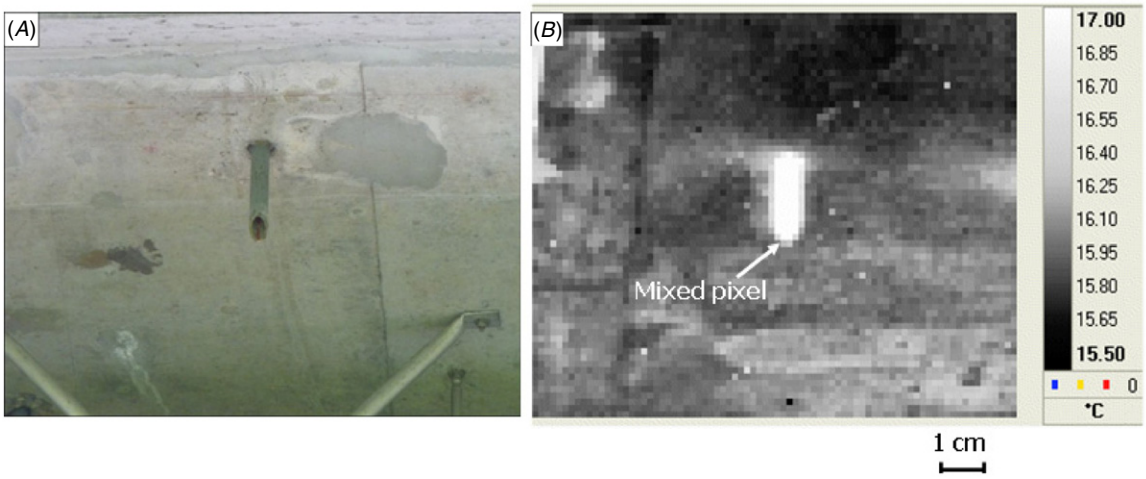


**Figure 4.** (*A*) Example of a frame acquired by FLIR camera. (*B*) The frame depicts a metal object (steel pipe) solidly cemented into the bridge structure that was used as a target to observe the thermal oscillation caused by the heavy vehicle traffic on the bridge. The white arrow indicates the mixed pixel (i.e. background and pipe) used for calculating the oscillation frequencies. The spatial resolution of a pixel is 18 mm.

scene. Furthermore, the accuracy, in terms of displacement measurement, of this method for the controlled experiment was calculated using the noisy oscillations (see figure 3(*C*)) starting from 7 s after the impact to the end of the measurement, i.e. when the beam oscillations stopped. The accuracy value was 1 mm, and was calculated with a distance of 40 m between the camera and target and a pixel IFOV of 1.2 mrad. This value is 45 times below the value of the maximum values of the amplitude oscillation observed during the heavy loading impact.

## 4. Data acquisition and results

The in-field measurements in Zurich lasted four days from 16 May to 19 May. They were characterized by the joint application of different electromagnetic sensors to define the state of health of the bridge. Among the sensors applied, IBIS-S system and FLIR thermal camera were first separately applied to perform some tests and measure specific parameters of the bridge. After that, also taking into account the results obtained during the controlled experiment performed in Montagnole, we decided to dedicate one day of measurements to the joint application of IBIS-S and FLIR camera for studying the dynamic characteristics of the Sihlhochstrasse Bridge.

### *4.1. IBIS-S sensor*

IBIS-S measurements were carried out from 16 May to 18 May. On the first day, some tests to understand if some corner reflectors must be placed on the structure were performed. These tests allowed us to assess that the installation of corner reflectors was not necessary due to the good backscatter intensity of the bridge.

Indeed, due to the geometrical characteristics of the bridge, we decided to use as a corner reflector, a natural corner of the infrastructure formed by the deck (see figure 1(*D*)). The IBIS-S system was installed on a tripod and placed on the ground on a pedestrian lane parallel to the main axis of the bridge.

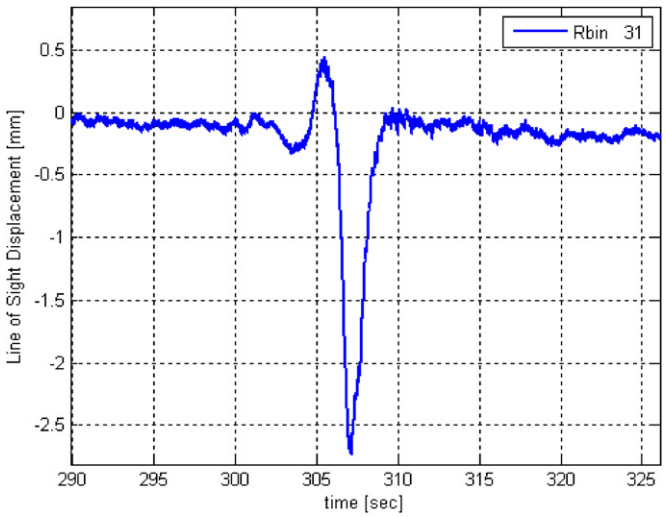


**Figure 5.** Example of LOS displacement recorded during the transit of a heavy vehicle, Rbin 31 (i.e. range bin 31) means that the sensor was 15 m distance from the observed point of the bridge, since the IBIS-S range resolution is 0.5 m.

On the last day, the IBIS-S system was placed in front of the Sihlhochstrasse Bridge at 15 m distance (range bin 31, see figure 5) with a LOS angle $\theta = 30^{\circ}$, and measurements were carried out together with the thermal camera. Each IBIS-S acquisition had a duration of about 20 min with a sampling frequency of 200 Hz.

For each acquisition, data were processed by using the commercial IBIS DATAVIEWER software that gives the displacement time histories from the data acquired by the IBIS-S radar sensor. On 18 May, the largest LOS displacement of 2.7 mm was measured during the transit on the bridge of a heavy vehicle (see figure 5). Assuming that this largest oscillation of the bridge was along the vertical component

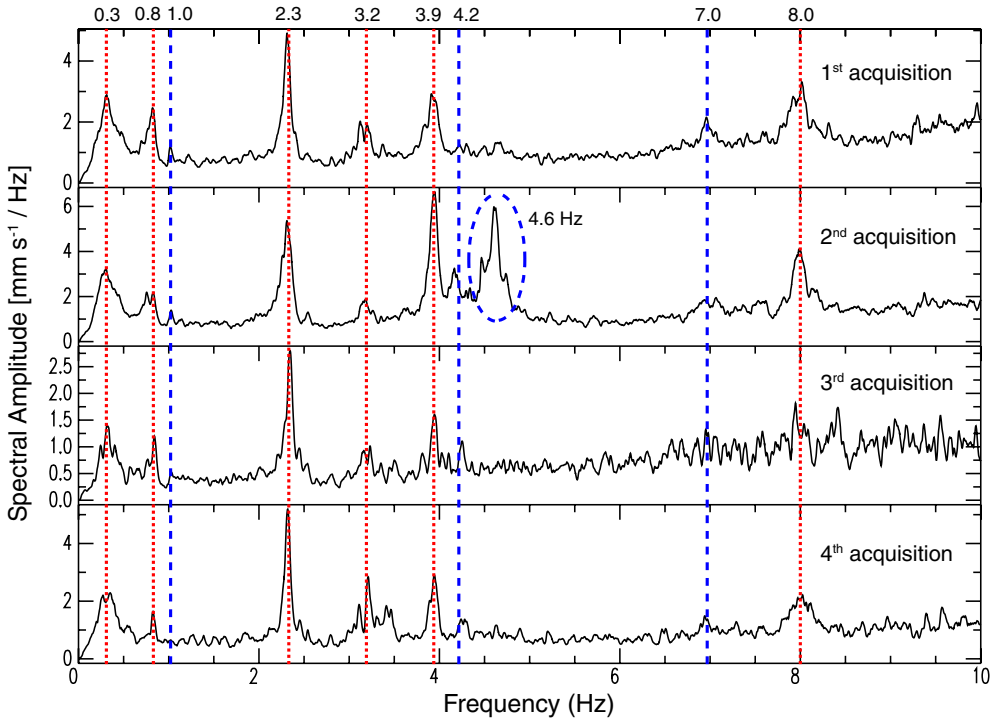


**Figure 6.** Fourier spectra in the frequency range 1–10 Hz related to four different acquisitions of the Sihlhochstrasse Bridge vibrations due to traffic excitations. All the measurements were performed on 18 May. Some resonant frequencies (dotted lines) are well recognizable in all acquisitions, while other frequency peaks (dashed lines) are evident only for some acquisitions or have small amplitudes.

(due to the vertical load exerted by the vehicle), from equation (4) and considering that $\theta = 30^{\circ}$, we found that it was 5.4 mm.

Afterwards, the discrete Fourier transform (DFT) was computed in order to assess the most important resonant frequencies of the structure. The mean and the linear trends were removed from all the displacement time histories, and the derivative was applied before applying the DFT. The obtained spectra are reported in figure 6, where it is possible to observe a series of peaks from 0.3 to 8.0 Hz. Some resonant frequencies (dotted lines in figure 6) are well recognizable in all acquisitions, whereas other frequency peaks (dashed lines in figure 6) are evident only for some acquisitions or have small amplitudes, as for the peak at 1.0 Hz.

### *4.2. FLIR thermal camera*

The methodology set up and optimized for the Montagnole controlled experiment was applied for the real case of the Sihlhochstrasse Bridge in order to test the efficiency of the method developed under controlled experiment for assessing the structure vibrations by high thermal frequency imaging acquisitions. The main differences between the controlled and real cases are due to the heavy loading impacting on the structure that for the controlled experiment was a heavy iron ball of 5 tons dropped from a maximum altitude of 5 m, while for the real case corresponded to the vehicles and in particular to heavy trucks in transit through the bridge. Further analysis and tests of the proposed methodology will also consider the decomposition of the displacement by using the real geometry of the experimental setup that for this case study was not included.

For this study, the LWIR camera was applied by using the following configuration: a sub-windowing mode of 80 $\times$ 64 frames thus allowing 200 FPS and 150 $\mu$s of integration time. The spatial resolution of a pixel is 18 mm, as also indicated in figure 4. The field measurement campaign was performed between 17 May and 19 May 2011 under clear sky conditions. The measuring sessions were executed in different sets of acquisitions according to the heavy traffic loadings on the bridge. The FLIR camera used for the Sihlhochstrasse test site was located on the ground installed on a tripod on a secondary pedestrian lane running parallel to the bridge in order to ensure the covering of the area of interest of the bridge structure (figure 1).

The high-frequency FLIR thermal acquisitions were performed at 200 Hz (the same as the IBIS-S sensor) to determine the oscillations of the bridge structure due to heavy traffic loading. The use of high-frequency thermal imagery gives the opportunity of measuring oscillation characteristics. For this test site, the TIR camera was positioned close to the IBIS-S sensor for synchronized acquisitions and to compare and analyse a different sensing technology for the structure vibration frequency on the same target area. The camera has been pointed to a steel pipe cemented into the bridge structure and of higher temperature with respect to the concrete background to measure the oscillation frequency of the pipe (figure 4(*A*)).

High-frequency radiance measurements were conducted for a period of 2 h in order to observe different solicitations of the structure due to cars and trucks on the bridge.

The thermal camera radiance imagery acquisitions were used to calculate the bridge oscillation frequency as derived

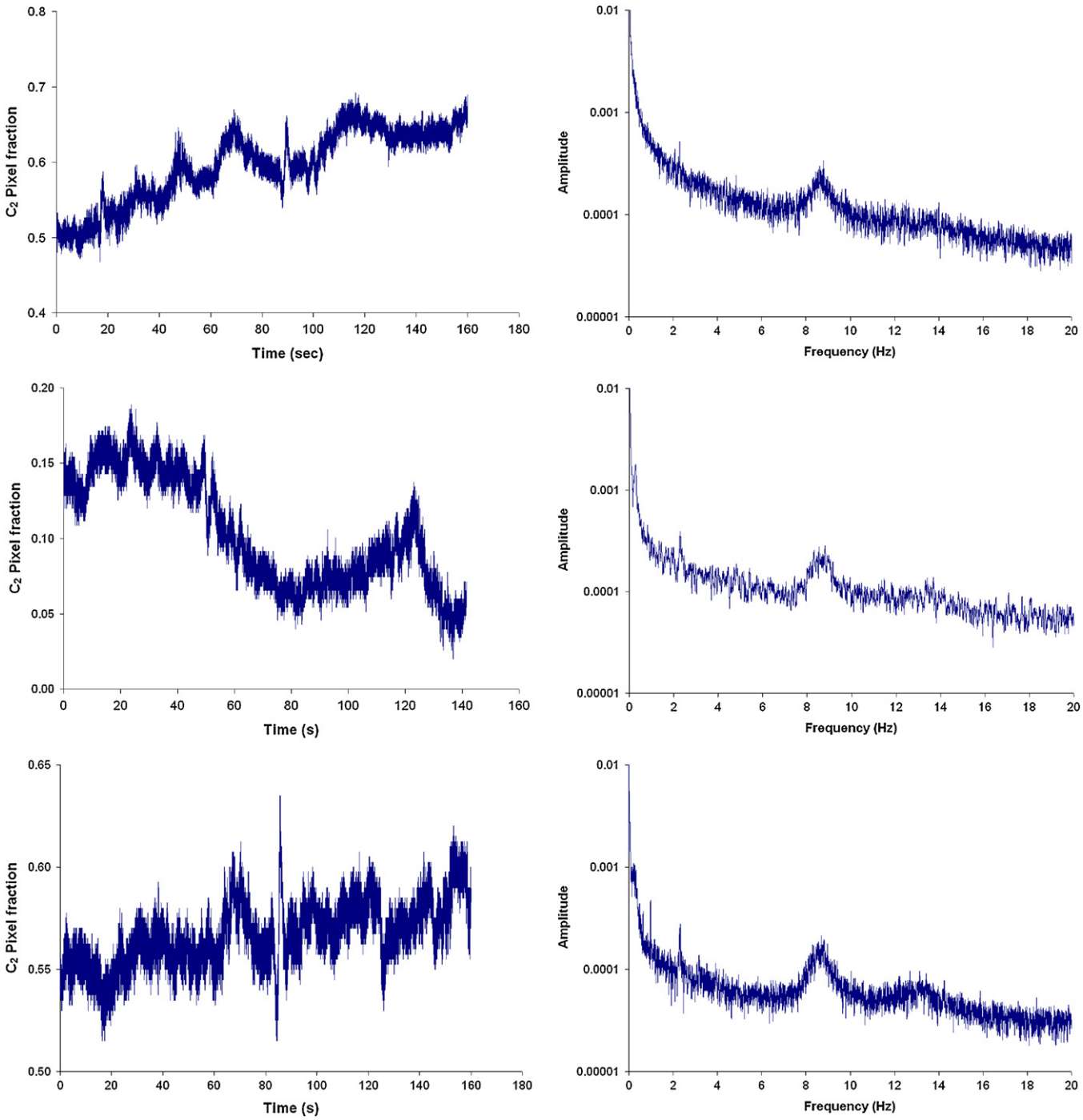


**Figure 7.** Left: graphs of the $c_2$ pixel fraction values calculated for the FLIR camera acquisitions on three registered oscillations due to heavy truck loadings on the Sihlhochstrasse Bridge. Right: the relative FFT amplitude (depicted in logarithmic scale only for visualization purposes) calculated for the same files (i.e. files 134, 136 and 137, respectively, from top to bottom).

from the difference between the cement structure of the bridge radiance and the pipe radiance (figure 4(*B*)).

The results of three TIR data acquisitions are presented, where the IRT sequence portions allow good identification of the structure oscillation frequencies due to heavy truck loadings and that were recorded at the same time and position as the IBIS-S sensor. Figure 7 (left) shows the $c_2$ pixel fraction values calculated for the FLIR camera acquisitions due to heavy truck loadings (i.e. files 134, 136 and 137, respectively, from top to bottom), while figure 7 (right) displays the relative FFT amplitude (depicted on the logarithmic scale only for visualization purposes). By analysing the FFT graphs, it is possible to isolate the oscillation frequencies of the most significant FFT coefficients that are shown in table 1.

The FFT results highlight that all three acquisitions show resonant frequencies at 2.3 and 8.7 Hz, whereas acquisitions 136 and 137 also show a resonant frequency at 0.3 Hz.

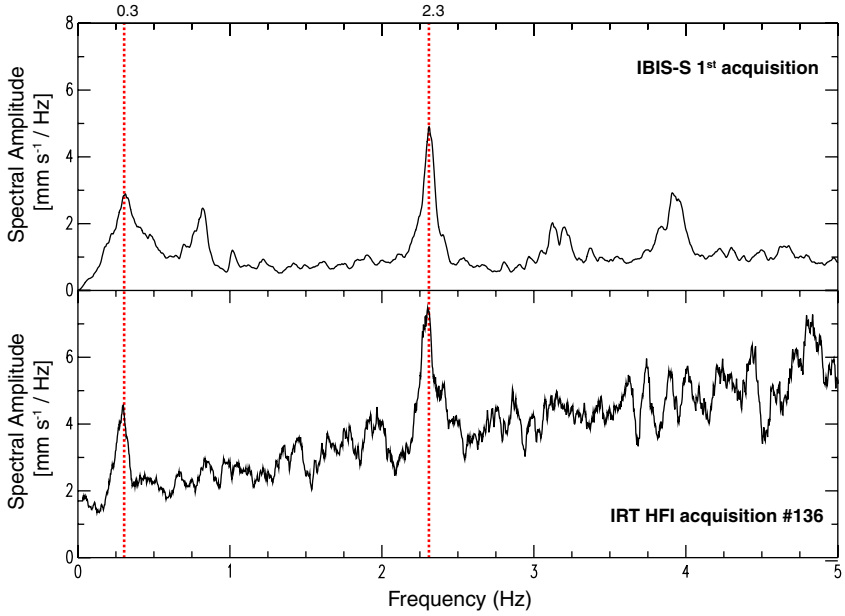


**Figure 8.** Comparison between the Fourier spectrum obtained from the derivative of the IBIS-S data (first acquisition) and the Fourier spectrum obtained from the derivative of the IRT HFI camera data (file 136). Dotted lines indicate the resonant frequencies commonly identified by both sensors. These frequencies could be related to vertical oscillations of the Sihlhochstrasse Bridge.

**Table 1.** Resonant frequencies as derived by the FFT of the thermal camera (IRT) high-frequency images.

| IRT HFI acquisition (file number) | Measured frequencies (Hz) | | | |
|---|---|---|---|---|
| No. 134 | – | – | 2.3 | 8.7 |
| No. 136 | 0.3 | – | 2.3 | 8.7 |
| No. 137 | 0.3 | 1.0 | 2.3 | 8.7 |

**Table 2.** Resonant frequencies measured by the HFI thermal camera and the IBIS-S radar sensor. Frequencies not observed in all acquisitions or measured by both the sensors without a stable common value are highlighted in grey.

| Sensor | Measured frequencies (Hz) | | | | | | | | |
|---|---|---|---|---|---|---|---|---|---|
| HFI thermal camera | 0.3 | – | 1.0 | 2.3 | – | – | – | – | 8.7 |
| IBIS-S radar sensor | 0.3 | 0.8 | 1.0 | 2.3 | 3.2 | 3.9 | 4.2 | 7.0 | 8.0 |

The most severe differences in the application of this technique between controlled conditions (i.e. laboratory controlled cases) and real cases, such as the Sihlhochstrasse Bridge, are related to the impulsive solicitation of the structure and its magnitude that allow better identification of the resonance frequencies. This difference is stressed by the difficulty in identifing the resonance frequencies in the real case; in fact, the amplitude of some of the identified frequencies is at the edge of noise.

### *4.3. Comparison of the FLIR camera and the IBIS-S sensor results*

Figure 6 highlights a series of resonant frequencies obtained by analysing the Fourier spectra of the IBIS-S acquisitions, while the comparison between the spectra obtained by the two different sensors in the frequency range 0–5 Hz is presented in figure 8. Moreover, in table 2, all the frequencies achieved by the two sensors are summarized. The comparison (figure 8) shows that there are two clear common resonant frequencies at 0.3 and 2.3 Hz, while frequencies at 0.8, 3.2 and 3.9 Hz well recorded by the IBIS-S instrument are not visible on the FLIR camera spectra.

Considering only the IBIS-S spectra, it is very difficult to distinguish between the frequencies related to vertical movements and those related to the horizontal ones. This is because the LOS angle was $\theta = 30°$; hence, from equation (4) the projection of the vertical oscillation of the bridge along the LOS was one half the nominal value and it cannot be considered negligible. On the other hand, the FLIR thermal camera measures oscillations projected in the plane orthogonal to the LOS and can be used to solve the problem.

Indeed, due to the typology of excitation (principally traffic load), the vertical oscillations of the bridge can be considered much larger and more important than those along the transversal and longitudinal directions, and so the two frequencies recorded by the FLIR thermal camera at 0.3 and 2.3 Hz should be related to the oscillation along this direction. For the same reason, it is possible to suppose that frequencies at 0.8, 3.2 and 3.9 Hz could be associated with horizontal oscillations, even if it may also be possible that they are below the noise level in the FLIR camera spectrum and cannot be evaluated by that sensor.

Further measurements should be carried out to better assess all the resonant frequencies, in particular those well observed by only the IBIS-S instrument that could be related to vertical oscillations of the bridge (if they are also detected by the thermal camera in forthcoming measurements). Finally, we should deepen the knowledge about the resonant frequencies

not observed in all acquisitions or measured by both the sensors without a stable common frequency value (see table 2).

## 5. Conclusions and discussions

This paper reports the results obtained by the combined application of the IBIS-S sensor and the FLIR camera to study the dynamic behaviour of the Sihlhochstrasse Bridge in Zurich, Switzerland.

Although the two techniques are based on different physical principles, they both can provide information about the displacement time histories and resonant frequencies of the investigated structure, which are comparable and can be integrated. In particular, the IBIS-S system obtains this information from the backscattering of emitted microwaves with a sensitivity of 0.01–0.02 mm comparable to commercial contact sensors (Pieraccini *et al* 2008), while the FLIR camera gets the same information from radiance measurements with a sensitivity of 1 mm.

Considering the way that both sensors work, it is easy to understand why the data can be integrated. The IBIS-S sensor provides valuable information along the LOS; thus, the measured resonant frequencies can be mainly associated with the displacement occurred along that direction. However, if the LOS of the sensor does not correspond to the main oscillation direction of the investigated structure, the frequencies measured can be associated with both vertical and horizontal components of the displacement.

The FLIR camera allows the displacement to be measured to its LOS. So, this means that if the two sensors look at the object from the same position and with the same angle, the information obtained is complementary and provides indications on the displacements in mutually orthogonal directions.

The results presented in this study provide only preliminary information about the joint application of the FLIR camera and the IBIS-S sensor for the evaluation of the dynamic behaviour of the Sihlhochstrasse Bridge. The survey performed cannot provide information about any damage of the structure because the deterioration is related to changes over time of resonant frequencies; hence, monitoring of the structure is necessary for a long period of time. Anyway, this joint application is very promising and can be considered very encouraging for the development of a new technological approach that will allow 2D SHM of infrastructures. In fact, this study demonstrates that the joint use of such techniques provides the displacement time histories of the monitored structure and the evaluation of its resonant frequencies along orthogonal directions.

The remote sensing character of the two applied techniques makes them particularly suitable for the study of structures located in areas affected by natural hazard phenomena, not easily accessible also for security reasons, and also to monitor cultural heritage buildings (Atzeni *et al* 2010) for which some conventional techniques are considered invasive. Another advantage of this approach is related to the measurement of the seismic ambient noise, which is very powerful in cases where it is not possible to perform invasive and/or expensive active dynamic analyses (e.g., by using a vibrodyne).

Obviously, their reliability needs further experiments focused on laboratory and field measurements together with standard contact sensor (such as accelerometers). After these experiments, it will be possible to evaluate the particle motion of the investigated structure that can be used by engineers, in addition to the resonant frequency information, to estimate its modal shapes.

## Acknowledgments

The research leading to these results has received funding from the European Community's Seventh Framework Programme (FP7/2007-2013) under grant agreement no. 225663 Joint Call FP7-ICT-SEC-2007-1, in the framework of the research project 'Integrated System for Transport Infrastructure surveillance and Monitoring by Electromagnetic Sensing' (ISTIMES).

## References

Ali D, Amir G, Wayne S T R, Kamran G and Sabu J 2012 Utilising microstrip patch antenna strain sensors for structural health monitoring *J. Intell. Mater. Syst. Struct.* **23** 169–82

Atzeni C, Bicci A, Dei D, Fratini M and Pieraccini M 2010 Remote survey of the leaning tower of Pisa by interferometric sensing *IEEE Geosci. Remote Sens. Lett.* **7** 185–9

Brown J R and Hamilton H R 2010 Quantitative infrared thermography inspection for FRP applied to concrete using single pixel analysis *Constr. Build. Mater.* at press (doi:10.1016/j.conbuildmat.2009.12.016)

Chang P C, Flatau A and Liu S C 2003 Review paper: health monitoring of civil infrastructure *Struct. Health Monit.* **2** 257–67

Cunha A and Caetano E 1999 Dynamic measurements on stay cables of cable-stayed bridges using an interferometry laser system *Exp. Tech.* **23** 38–43

Doebling S W, Farrar C R, Prime M B and Shevitz D 1996 Damage identification and health monitoring of structural and mechanical systems from changes in their vibration characteristics: a literature review *Report LA-13070-MS Los Alamos National Laboratory* (available at http://institute.lanl.gov/ei/shm/pubs/lit_review.pdf)

Farrar C R, Darling T W, Migliori A and Baker W E 1999 Microwave interferometers for non-contact vibration measurements on large structures *Mech. Syst. Signal Process.* **13** 241–53

Farrar C R and Worden K 2007 An introduction to structural health monitoring *Phil. Trans. R. Soc.* A **365** 303–15

Gentile C 2010 Application of microwave remote sensing to dynamic testing of stay-cables *Remote Sens.* **2** 36–51

Gentile C and Bernardini G 2008 Output-only modal identification of a reinforced concrete bridge from radar-based measurements *NDT & E Int.* **41** 544–53

Gentile C and Bernardini G 2009 An interferometric radar for non-contact measurement of deflections on civil engineering structures: laboratory and full-scale tests *Struct. Infrastruct. Eng.* **6** 521–34

Ha H, Han S and Lee J 2012 Fault detection on transmission lines using a microphone array and an infrared thermal imaging camera *IEEE Trans. Instrum. Meas.* **61** 267–75

Henderson F M and Lewis A J 1998 *Manual of Remote Sensing: Principles and Applications of Imaging Radar* (New York: Wiley) p 866

Ko J M and Ni Y Q 2005 Technology developments in structural health monitoring of large-scale bridges *Eng. Struct.* **27** 1715–25

Lee J J and Shinozuka M 2006 A vision-based system for remote sensing of bridge displacement *NDT & E Int.* **39** 425–31

Li H N, Li D S and Song G B 2004 Recent applications of fiber optic sensors to health monitoring in civil engineering *Eng. Struct.* **26** 1647–57

Maierhofer C, Arndt R, Rollig M, Rieck C, Walther A, Scheel H and Hillemeier B 2006 Application of impulse-thermography for non-destructive assessment of concrete structures *Cem. Concr. Compos.* **28** 393–401

Malone R M, Celeste J R, Celliers P M, Frogget B C, Guyton R L, Kaufman M I, Lee T L and MacGowan B J 2005 Combining a thermal-imaging diagnostic with an existing imaging VISAR diagnostic at the National Ignition Facility (NIF) *Int. Soc. Opt. Eng.* **5874** 1–8

Martire G, Faggiano B, Mazzolani F M, Zollo A and Stabile T A 2010 Seismic analysis of a SFT solution for the Messina Strait crossing *Proc. Eng.* **4** 303–10

Martire G, Faggiano B, Mazzolani F M, Zollo A and Stabile T A 2012 A comprehensive study on the performance of submerged floating tunnels during severe seismic events *Proc. 7th Int. Conf. on Behaviour of Steel Structures in Seismic Areas (STESSA)* pp 523–29

Minardo A, Bernini R, Amato L and Zeni L 2012 Bridge monitoring using Brillouin fiber-optic sensors *IEEE Sens. J.* **12** 145–50

Mucciarelli M, Bianca M, Ditommaso R, Vona M, Gallipoli M R, Giocoli A, Piscitelli S, Rizzo E and Picozzi M 2011 Peculiar earthquake damage on a reinforced concrete building in San Gregorio (L'Aquila, Italy): site effects or building defects? *Bull. Earthq. Eng.* **9** 825–40

Nickitopoulou A, Protopsalti K and Stiros S 2006 Monitoring dynamic and quasi-static deformations of large flexible engineering structures with GPS: accuracy, limitations and promises *Eng. Struct.* **28** 1471–82

Palombo A, Pignatti S, Perrone A, Soldovieri F, Stabile T A and Pascucci S 2011 Noninvasive remote sensing techniques for infrastructures diagnostics *Int. J. Geophys.* 204976

Pascucci S, Bassani C, Palombo A, Poscolieri M and Cavalli R 2008 Road asphalt pavements analysed by airborne thermal remote sensing: preliminary results of the Venice highway *Sensors* **8** 1278–96

Picozzi M *et al* 2010 Wireless technologies for the monitoring of strategic civil infrastructures: an ambient vibration test on the Fatih Sultan Mehmet suspension bridge in Istanbul, Turkey *Bull. Earthq. ECng.* **8** 671

Pieraccini M, Fratini M, Parrini F, Atzeni C and Bartoli G 2008 Interferometric radar vs accelerometer for dynamic monitoring of large structures: an experimental comparison *NDT & E Int.* **41** 258–64

Pieraccini M, Fratini M, Parrini F, Macaluso G and Atzeni C 2004 Highspeed CW step-frequency coherent radar for dynamic monitoring of civil engineering structures *Electron. Lett.* **40** 907–8

Pieraccini M, Parrini F, Fratini M, Atzeni C, Spinelli P and Micheloni M 2007 Static and dynamic testing of bridges through microwave interferometry *NDT & E Int.* **40** 208–14

Pines D and Aktan A E 2002 Status of structural health monitoring of long-span bridges in the United States *Prog. Struct. Eng. Mater.* **4** 372–80

Proto M *et al* 2010 Transport infrastructure surveillance and monitoring by electromagnetic sensing: the ISTIMES project *Sensors* **10** 10620–39

Rehm R, Walther M, Schmitz J, Fleißner J, Fuchs F, Ziegler J and Cabanski W 2005 As/GaSb superlattice focal plane arrays for high-resolution thermal imaging *Proc. SPIE* **5957** 595707

Rödelsperger S, Läufer G, Gerstenecker C and Becker M 2010 Monitoring of displacements with ground-based microwave interferometry: IBIS-S and IBIS-L *J. Appl. Geod.* **4** 41–54

Taylor J D 2001 *Ultra-Wideband Radar Technology* (New York: CRC Press) p 424